

New Calibration in Cycles 23-26 & Detector Monitoring Results over the WFC3 Lifetime

J. Mack & the WFC3 Team
September 26, 2018

ABSTRACT

The annual WFC3 calibration program is designed to monitor the performance of both UVIS and IR channels. Additional ‘special’ calibrations are proposed each cycle to support new observing strategies and initiatives, such as scanned imaging, or to further understand known detector issues, such as IR persistence. Each program is prepared with the usage of WFC3 in mind, in order to provide the best possible calibration data and reference files for the approved scientific programs each cycle. This report highlights supplemental calibration acquired over the last four years and provides a summary of all results to date for routine monitoring programs, with a comprehensive set of links to Instrument Science Reports listed by topic.

I. Introduction

The Wide Field Camera 3 (WFC3) is a 4th generation instrument on the Hubble Space Telescope (HST) installed during the final HST servicing mission (SM4) in May 2009, replacing the Wide Field Planetary Camera 2 (WFPC2) at the center of the HST focal plane. With panchromatic wavelength coverage from 200 nm to 1700 nm, WFC3 continues to be the primary camera used for science observations, with ~50% of the total HST orbit allocation.

WFC3 consists of two independent cameras: the UV/Visible channel (UVIS) and the near-infrared channel (IR). The UVIS channel is comprised of two 4096 x 2051 pixel CCD detectors, each with a plate scale of ~0.0396"/pixel. The combined field of view is 162" x 162", with a small

31-pixel gap between the two detectors. The CCDs are thinned and backside-illuminated to improve their sensitivity to UV light, and they cover a wavelength range from 200-1000 nm. The UVIS channel is equipped with 62 broad, medium, and narrow band filters and one UV grism. Forty-two filters cover the full detector field of view, and the remaining 20 filters are organized into 5 sets of “quad” filters, each set containing a unique spectral element on each of the 4 amplifiers. The nominal operating temperature of the UVIS detector is -83 C.

The IR channel is a single 1024 x 1024 HgCdTe detector array, of which the central 1014 x 1014 pixels are used for imaging. This channel operates at a nominal temperature of 145 K and covers the near-infrared wavelength range of the spectrum between 800 and 1700 nm. The detector field of view is 136” x 123”, with a plate scale of ~0.128”/pixel. The IR channel is equipped with 15 broad, medium and narrow band filters, two grisms, and one ‘blank’ filter slot.

A more detailed description of the instrument performance, along with considerations for designing an observing proposal, may be found in the WFC3 Instrument Handbook (Dressel 2018). A discussion of WFC3 data products, including instructions for recalibration, may be found in the WFC3 Data Handbook (Gennaro et al. 2018).

The initial calibration of WFC3 was performed during ground testing under simulated orbital conditions. Shortly after launch, on-orbit observations were used to assess the performance of the two channels during Servicing Mission Orbital Verification (SMOV). As with all active HST instruments, the WFC3 team maintains an annual calibration program to monitor the behavior of both UVIS and IR channels and to provide the best calibration data for the approved scientific programs. In each cycle, calibration observations begin scheduling in early November and run for ~12 months. The latest results from these calibration programs are documented as Instrument Science Reports (ISRs) which are available from the ‘WFC3 ISRs’ webpage at <http://www.stsci.edu/hst/wfc3/documents/ISRs>.

Each year, the WFC3 calibration plan is designed to:

- monitor the health of the instrument (throughput, gain, hysteresis, bad/hot pixels, sink pixels, charge transfer efficiency (CTE), post-flash LED stability, filter transmission, status of the channel select mechanism (CSM), number of IR blobs, and the wavelength and flux stability of the grisms)
- maintain and update reference files used by the calwf3 reduction pipeline (biases, darks, flats, linearity, CTE traps, anomalous QE pixels, post-flash)
- support new initiatives and obtain supplemental (non-routine) calibration data.

Details on calibration activities dating back to ground testing (2004 - 2008), orbital verification (2009), and later for in-flight monitoring in Cycles 17 through Cycle 26 (2010-2019) may be found on the ‘WFC3 Calibration Plan’ webpage <http://www.stsci.edu/hst/wfc3/calibration>. This allows for a direct comparison of calibration in the current cycle with that done in prior cycles.

This report highlights WFC3 calibration data obtained over the past four years, spanning Cycles 23 through 26. Prior calibration cycles are described in Sabbi et al. (2012, 2013, 2014, 2015), Deustua (2011), and Deustua et al. (2010). Metrics on the usage of WFC3 over time, relative to the other HST instruments, are provided in Section 2. Additional metrics on the use of various WFC3 modes for science observations and the total number of calibration orbits acquired in each cycle are provided. Section 3 highlights ‘new’ (non-routine) calibration designed to support new observing strategies or to further investigate known detector effects.

Section 4 describes the twenty-three routine calibration programs which are repeated each year to monitor the performance of the two WFC3 channels. These are categorized into seven different topics: UVIS Detector, CTE Characterization, IR Detector, Grisms, Photometry, Flat Fields, and Astrometry. The majority of these programs have executed every cycle since SMOV, and this section provides a comprehensive list of program IDs, details on the observing strategy, and a set of direct links to ISRs available on a given topic. Because the ISR webpage is not yet searchable by keyword, this compilation of references is provided for convenience to WFC3 users who wish to learn more about a given topic and how our knowledge has evolved (improved) over time.

II. WFC3 Metrics

HST Orbit Allocation by Instrument

Instrument usage metrics for General Observer (GO) programs may be found on the ‘HST Selection Statistics’ webpage at <http://www.stsci.edu/hst/metrics/SelectionStats>. The percentage of HST orbits allocated to the various instruments as a function of observing cycle is shown in Figure 1. This figure was generated using the combined set of ‘GO Instrument Usage’ text files provided for each observing cycle, beginning in Cycle 10 at year 2001.5 (just prior to the installation of ACS) and ending in Cycle 25 which extends through year 2018.8. These metrics reveal several notable events in the history of the observatory:

- ACS was installed in March 2002 to support Cycle 11 science observations, replacing the Faint Object Camera. At this time, the usage of STIS went down by roughly half, from ~60% in Cycle 10 to ~27% ($\pm 4\%$) in Cycles 11-13. At this time, the usage of WFPC2, the prior main imaging camera, dropped by nearly a factor of 10.
- The STIS detector failed in August 2004 at the beginning of Cycle 13, and the orbit allocation for Cycles 14-16 is 0%. STIS was successfully repaired in SM4 to support Cycle 17 science observations. However, with the installation of COS (replacing COSTAR) and WFC3 (replacing WFPC2), the use of STIS went down by roughly half again to ~13% ($\pm 5\%$) of the total orbit allocation, compared to Cycles 11-13. Between Cycles 17-25, the fraction of COS and STIS observations remain comparable to one another and roughly steady with time.

- A dip in the usage of ACS in Cycle 16 is due to the failure of the side-2 electronics in early 2007 impacting the operation of the WFC and HRC detectors, while the SBC remained in use. This period corresponds to a sharp increase in WFPC2, NICMOS, and FGS observations for that cycle when science observations were reallocated to the other operating HST instruments.
- The NICMOS detector failed in mid-2008, resulting in 0% of the orbit allocation for Cycles 17 and beyond.
- WFC3 was installed in May 2009 at the center of the HST focal plane. Since that time, the usage of ACS in Cycles 17-25 has been $\sim 21\%$ ($\pm 4\%$), less than half of its prior usage compared to Cycles 11-15 when it made up $\sim 56\%$ ($\pm 10\%$) of the orbit total. WFC3 usage has remained roughly stable at $\sim 48\%$ ($\pm 5\%$) of the total orbit allocation since it was installed in HST, and it remains the main instrument requested for GO science programs.

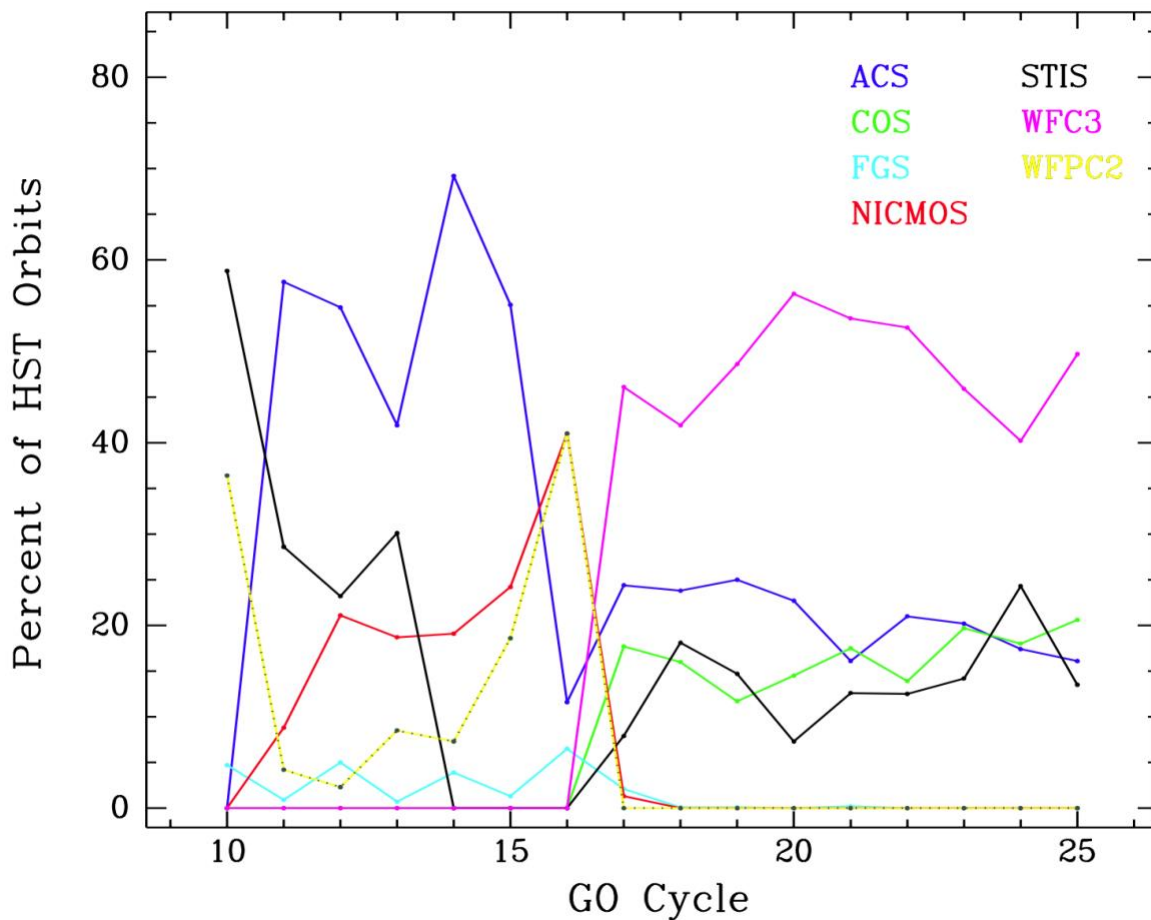


Figure 1: HST orbit allocation by instrument for GO programs between Cycles 10 and 25 (years 2001.5 - 2018.8). ACS was installed just prior to Cycle 11 and WFC3 prior to Cycle 17, making up the majority of observations for each respective time period.

WFC3 Usage for Science Observations

Statistics on the usage of the two WFC3 channels, based on Phase II GO proposal submissions from Cycles 17 through 25, are available from the ‘WFC3 Instrument Usage’ webpage at <http://www.stsci.edu/hst/metrics/SiUsage/WFC3>. A text file with the ‘WFC3 Total Usage’ is provided for each cycle and includes statistics on prime, SNAP, and coordinated parallel observations. These metrics were used to create Table 1, which lists usage statistics for the last four observing cycles as a percentage of the total WFC3 exposure time (in seconds). Columns 3 and 4 give the percentage of UVIS and IR prime observations, respectively, and these columns sum to 100%. The values given in parentheses are percentages for total usage, which includes prime, SNAP, and coordinated parallel observations. As in prior cycles, the IR detector continues to be the primary WFC3 channel requested by observers, with exception of Cycle 24 which had a large number of UVIS coordinated parallels.

Additional metrics, including usage by various Phase II keywords (FILTER, APERTURE, SAMPSEQ, NSAMP, and PATTERN), may also be found on this webpage for the UVIS and IR channels. For example, the fraction of WFC3 exposure time allocated to support the HST ‘UV Initiative’ is listed in column 5 and was computed from prime usage metrics by FILTER. This special initiative, in place since Cycle 21 and continuing into Cycle 26, was developed in recognition of the finite lifetime of Hubble and its unique capabilities in accessing the ultraviolet (UV) portion of the electromagnetic spectrum. It applies HST instrument modes (with central wavelength <3200 Angstroms). For WFC3, this includes UVIS imaging in the UV filters, F218W, F225W, F275W, F280N, FQ232N, FQ243N, F200LP, F300X) and spectroscopy with the G280 grism. More details for the upcoming GO cycle may be found on the ‘HST Special Initiatives’ webpage: <https://hst-docs.stsci.edu/display/HSP/HST+Cycle+26+Special+Initiatives>. The percentages listed in Table 1 indicate that the use of WFC3 for UV observations does not appear to have increased as a result of this initiative, with ~7% ($\pm 1\%$) of the total WFC3 time allocation over the last four GO cycles.

IR spectroscopy remains a popular mode for WFC3 science observations, with roughly 20% of the prime usage over the past four cycles, as reported in column 6. Spatial scans have gained popularity in Cycles 24 and 25, with usage increasing by a nearly a factor of three compared to Cycles 22 and 23 when it was still a relatively new observing strategy (see column 7). Scans are especially useful for programs that wish to do high-precision astrometry or for those that require very high signal-to-noise, such as time-series observations of exoplanet transits.

Sabbi et al. (2015) report WFC3 usage in Cycles 17 through 22 as a percentage of the total number of exposures. (Prior to Cycle 22, usage metrics based on the total exposure time were not yet available.) Compared to the total exposure time, statistics based on the number of exposures tend to overestimate usage of the IR detector, since grism programs typically acquire a short, direct imaging exposure just prior to spectroscopic observations. Thus Sabbi’s usage values for the IR detector in Cycle 22 are slightly larger than the values given in Table 1.

Table 1. WFC3 usage for science observations over the past four cycles, expressed as a percentage of the total WFC3 exposure time (in seconds). Column 2 lists the cycle boundaries in decimal years, and columns 3 and 4 give the percentage of UVIS and IR observations allocated for prime WFC3 observations. (These two columns sum to 100%.) For comparison, the total allocation, a combination of prime, SNAP, and coordinated parallels, is listed in parentheses below the prime usage. Column 5 gives prime usage for UV observations (imaging and spectroscopy) with respect to the total WFC3 allocation. Prime usage allocated for IR spectroscopy (G102 and G141) and spatial scans (UVIS and IR) is listed in columns 6 and 7.

GO Cycle	Cycle Boundaries (decimal years)	UVIS Prime Usage (Total Usage)	IR Prime Usage (Total Usage)	UV Science	IR Grisms	Spatial Scans
25	2017.8 - 2018.8	46% (47%)	54% (53%)	6.5%	16.1%	10.1%
24	2016.8 - 2017.8	45% (54%)	55% (46%)	7.0%	22.6%	15.1%
23	2015.8 - 2016.8	35% (36%)	66% (64%)	5.8%	19.5%	5.5%
22	2014.8 - 2015.8	43% (44%)	57% (56%)	7.6%	19.4%	4.1%

WFC3 Usage for Calibration

A summary of calibration activities for to the various HST instruments dating back to Cycle 9 may be found on the ‘HST Calibration Plan’ webpage, available from <http://www.stsci.edu/hst/metrics/CalibrationPlan>. Figure 2 was taken directly from this page and shows the total number of external (top panel) and internal (bottom panel) calibration orbits allotted per instrument in each cycle. Additional metrics from the ‘Calibration Program Summary’ text file indicate that the percentage of HST external orbits allocated for calibration was the highest in Cycle 17 at ~13% of the total number of available external orbits. At this time, the telescope had two new instruments (WFC3 & COS) and two repaired instruments (ACS & STIS) which required detailed re-characterization. Since Cycle 17, the percentage of external orbits allocated for calibration has declined slightly from 6.7% of the total available external orbits in Cycle 18 to 4.5% in Cycle 25. (Internal calibration orbits are typically acquired during Earth occultation so do not directly impact the GO orbit allocation.)

The number of calibration orbits allocated to WFC3 in Cycles 22 through 26 is listed in Table 2. Columns 2 and 3 give the total number of external and internal orbits, respectively, and these are depicted as purple triangles in Figure 2. The number of orbits allocated for routine monitoring is

listed in columns 4 and 5, and these have remained roughly steady over the past 5 cycles. Columns 6 and 7 give the number of orbits allocated to support new calibration initiatives, and these (both external and internal orbits) continue to decline each cycle as the characterization of both detectors improves over time with additional in-flight data. A history of calibration activities over the lifetime of the instrument may be found on the ‘WFC3 Calibration Plan’ webpage at <http://www.stsci.edu/hst/wfc3/calibration>.

In addition to dedicated calibration orbits, the WFC3 team makes use of archival GO science observations to improve the detector calibration when possible. For example, an effort is currently underway to derive wavelength-dependent corrections to the IR spatial sensitivity (flat fields) by computing sky flats by co-adding deep exposures of sparse fields from in-flight data acquired over the past 9+ years.

Table 2. Orbits allocated for WFC3 calibration in Cycles 22 - 26. Columns 2 and 3 list the total number of external and internal calibration orbits, plotted as purple triangles in Figure 2. Columns 4 and 5 provide the number of external and internal orbits for routine monitoring, and columns 6 and 7 give the orbit totals for ‘new’ calibration initiatives. For orbit totals from Cycles 17 - 21, see Table 1 in Sabbi et al. (2015) or Figure 2 in this report.

CAL Cycle	Total External Orbits	Total Internal Orbits	Monitor External Orbits	Monitor Internal Orbits	‘New’ External Orbits	‘New’ Internal Orbits
26	55	1514	49	1512	6	2
25	60	1512	48	1509	12	3
24	69	1557	50	1522	19	35
23	98	1619	52	1551	46	108
22	113	1620	58	1509	55	111

III. New WFC3 Calibration Initiatives

In addition to the standard monitoring programs, which are discussed in Section 4, supplemental calibration data is acquired each cycle to support new WFC3 observing strategies or to gain a deeper understanding of known detector effects, such as CTE in the UVIS channel or persistence in the IR channel. A number of new calibration initiatives have been developed over the past four cycles since the last ‘Calibration Program’ ISR (Sabbi et al. 2015) was written. These new programs are listed in reverse-chronological order by cycle in the following text, with a one line description of the calibration goals.

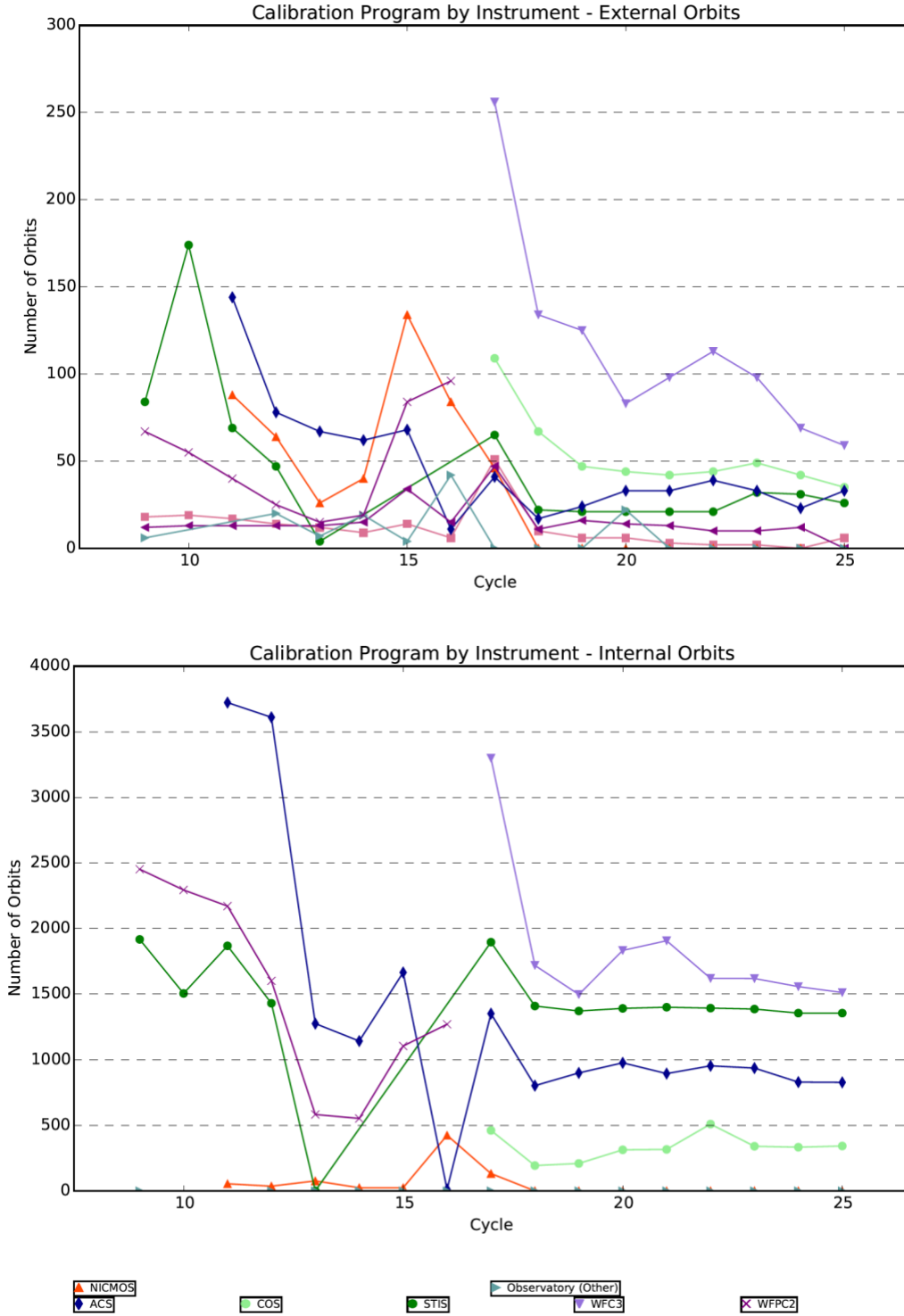


Figure 2: Calibration orbit allocation by HST instrument from Cycle 9 through Cycle 25 (decimal years 2001.5 - 2018.8). External orbits are shown in the top panel and internal orbits (typically scheduled during Earth occultation) in the bottom panel. These plots were obtained from the [HST Calibration Plan](#) metrics webpage.

The **Cycle 26** calibration plan begins in November 2018 and extends for one year (date range 2017.8 - 2018.8). Two new programs will supplement the standard detector monitoring programs. The goal of these programs will be:

- Cross-calibrating the HST focus derived from the routine OTA Focus monitor program (which obtains UVIS/F410M observations) with the focus values derived empirically from the UVIS PSF database, which has many more observations in the F606W filter
- Characterizing the decay of IR persistence at short time-scales ($t < 300$ sec), where the observed residual signal deviates from the current power-law model correction

The **Cycle 25** calibration plan (2016.8 – 2017.8) included two supplemental programs with the purpose of:

- Quantifying color terms in the UV filters and rechecking the absolute photometric calibration at the center of the detector with the UVIS2-M512C subarray, which has not been used for photometric monitoring since 2012 (in Cycle 19)
- Testing a strategy to mitigate IR persistence for time-series observations (repeated visits) by using the calibration lamp to fill charge traps just prior to an exposure

In **Cycle 24** (2015.8 – 2016.8), six supplemental programs provided additional calibration data to complement the standard detector monitoring. These were designed to achieve the following goals:

- Re-characterizing the 2014 UVIS pixel-based CTE model and verifying that the recommended post-flash level for science observations has not changed
- Evaluating the accuracy of this new pixel-based CTE model using observations of the Galactic bulge in order to determine the efficacy of the correction algorithm
- Updating the 2014 UVIS sink pixel map and measuring the shape and strength of these detector defects as a function of the total background
- Testing the precision of the IR count rate non-linearity correction for faint targets and determining whether the effect is wavelength-dependent, as was found for NICMOS
- Testing the IR absolute photometric calibration derived using faint standards and verifying that the inverse sensitivity values (zeropoints) agree with those derived from bright calibration standards

- Improving the spectrum of the white dwarf GRW+70D5824 in the CALSPEC database by obtaining additional STIS spectroscopy, allowing this target to be used a WFC3 flux standard for absolute calibration

The calibration plan for **Cycle 23** (2014.8 - 2015.8) included five special programs designed for:

- Studing amplitude variations in the IR persistence for a variety of exposure times and fluence levels
 - Developing a position-dependent persistence model and understanding how this effect can be ‘reactivated’ following bright exposures with the tungsten lamps
 - Improving the flux calibration of the -1st order of the IR grisms for spectroscopic observations of very bright targets
 - Computing filter-dependent distortion corrections for UVIS filters which were not observed in prior calibration cycles
 - Constraining the time-dependence of the UVIS charge-transfer efficiency in the serial (X) direction for improved high-precison astrometry
-

These supplemental programs are grouped by calibration topic in Table 3, rather than chronological order, in order to highlight areas of recent focus by the WFC3 team. While the monitoring programs fall into seven general categories (UVIS Detector, UVIS CTE, IR Detector, Grisms, Photometry, Flat Fields, and Astrometry), two unique categories are highlighted in Table 3. These include ‘PSF / Focus’, which is a new initiative for Cycle 26, and ‘Persistence’, which has been a topic of investigation over several prior calibration cycles. For the later topic, the observing strategy has changed significantly each cycle as the characterization of this IR detector effect continues to improve, so it is not listed with the monitoring programs.

The fifteen new programs are described in more detail in the following text and include: 1.) the purpose of each calibration, 2.) details of the observing strategy, and 3.) any related ISRs on each topic. More information on these new calibration initiatives may be obtained from the Phase II file by searching for the program ID from the ‘HST Program Status’ webpage at http://www.stsci.edu/hst/scheduling/program_information.

Table 3. WFC3 calibration in Cycles 23 through 26, listed in reverse chronological order by topic. These programs support new initiatives beyond the standard detector monitoring data obtained each cycle. Columns 2 - 4 list the calibration cycle, proposal ID, and title, and columns 5 - 6 give the number of external and internal orbits allocated for each program.

Topic	Cycle	ID	Program Title	External	Internal
PSF / Focus	26	15585	WFC3 Focus Cross-Calibration	4	0
Persistence	26	15581	WFC3 Short-term IR Persistence	2	2
	25	15400	Mitigating Persistence for Time-Series Observations	3	3
	23	14380	IR Persistence: Amplitude Variations	0	60
	23	14381	IR Persistence: Position Dependent Model	16	48
Photometry	25	15399	UVIS Supplemental Photometry: Color Terms & Revisiting M512C	2	0
	24	14868	Improved Precision, Wavelength Dependence of the IR Count Rate Non-Linearity	5	0
	24	14870	IR Zeropoint Linearity	2	0
	24	14871	Improved CALSPEC model for GRW+70D 5824	4	0
UVIS Detector	24	14879	UVIS Sink Pixel Map Update	0	20
UVIS CTE	24	14880	UVIS CTE Model Re-Characterization	0	15
	24	14881	UVIS CTE Pixel-Based Model Evaluation	2	0
Grisms	23	14388	WFC3 -1 st order IR grism calibration	2	0
Astrometry	23	14393	Astrometric Verification of Broad, Medium, Narrow, and Quad WFC3/UVIS Filters	30	0
	23	14394	Time-Dependence of X-CTE and Astrometry	4	0

1.) PSF / Focus

❖ WFC3 Focus Cross-Calibration: F410M to F606W

Purpose: Cross-calibrate the HST focus in two UVIS filters using interleaved exposures in F410M and F606W. This program supplements the existing CAL/OTA Focus program, which executes every 2 months in F410M and allows us to tie those observations to empirical focus values from the WFC3 PSF database which has many more F606W observations.

Description: The bimonthly HST/OTA Focus Monitor uses the UVIS filter F410M to take shallow subarray exposures of the sparse open cluster NGC188. Phase retrieval (PR) is performed on the stellar images to measure the focus of each exposure in equivalent secondary mirror despace. These focus measurements are used to track the evolution of the focus over months and years. Recent PR results have been combined with PR analysis of STIS parallel data in UVIS/F410M of a field near 47 Tucanae to relate the empirical PSF to the absolute focus. This calibration has been applied to additional F410M exposures to track focus evolution, but similar calibration of a more commonly used UVIS filter, F606W, can greatly improve our ability to perform this tracking. This program will observe a rich cluster with interleaved F410M and F606W exposures to perform the calibration accurately and efficiently. Four visits spread over Cycle 26 will sample the breathing curve over different ranges of focus. The visits are interspersed among the bi-monthly visits in the CAL/OTA Focus program to contribute to the tracking of focus trends using F410M.

IDs:	15585 (Cycle 26)
ISRs:	ISR 2012-14: Breathing, Position Drift, and PSF Variations on the UVIS Detector ISR-TEL-2010-03, Phase Retrieval to Monitor HST Focus: II. Results Post-SM 4 ISR-TEL-2010-01, Phase Retrieval to Monitor HST Focus: 1. WFC3 UVIS Software Implementation

2.) Persistence

❖ WFC3 Short-Term IR Persistence

Purpose: Persistence in the IR channel decays as a power law with time for $t > 300$ seconds. Using observations of the star cluster Westerlund 1 from program 14016, a tapering of the power law has been observed at short times. The analysis of those data is, however, limited to the darks; the external exposures suffer from too much crowding, making it difficult to measure the local background and the persistence signal on top of it. In order to truly exploit the externals and reach the shortest allowed times, a more compact target has been selected to provide a larger

“free” portion of the IR detector in order to obtain more accurate measurements of the sky background.

Description: This program consists of multiple multi-accum exposures of the planet Uranus in F127M, stepped by ~30 arcsec between exposures. By dithering the detector, the persistence in pixels stimulated in earlier exposures will be measured. The exposures are followed by a series of darks to measure the persistence. These darks extend for ~4000 seconds after the externals.

IDs:	15581 (Cycle 26)
ISRs:	ISR 2018-05: A characterization of persistence at short times in the WFC3/IR detector

❖ Mitigating Persistence for Time-Series Observations

Purpose: Mitigate the effect of persistence, the dominant systematic in time-series observations (TSOs), and enable the use of HST’s first orbit for TSO science.

Description: Persistence causes an increase in measured flux over time. The effect varies between the first HST orbit and subsequent orbits and is likely due to having multiple trap populations filling at different rates. Current TSOs exclude the first HST orbit from their analysis, but this process could change if the detectors were preconditioned prior to the first HST orbit and during Earth occultation. This program is designed to continuously illuminate the detector using the internal Tungsten lamp with F140W (1450 e⁻/s) during Earth occultation prior to the first exposure and between consecutive exposures. The detector read pattern during occultation would be selected to achieve the same fluence per integration with the Tungsten lamp as would be seen from the target, with a goal of 25-30 Ke⁻. Observations of GJ 1214 (*outside of transit*) are obtained over 3 contiguous orbits using the G141 grism. Ten of the fifteen GJ 1214 observations from GO program 13021 (PI: Bean) use the same settings as this program and serve as an ideal baseline for comparison.

IDs:	15400 (Cycle 25)
ISRs:	ISR 2014-14: Attempts to Mitigate Trapping Effects in Scanned Grism Observations of Exoplanet Transits with WFC3/IR

❖ IR Persistence: Amplitude Variations

Purpose: Improve the current persistence model by obtaining data that would allow the creation of persistence correction ‘flats’ for a variety of exposure times and fluence levels.

Description: The IR detector shows a faint afterglow from prior observations when the detector has been exposed to levels that reach saturation. A model of persistence has been developed that depends upon the degree of saturation of each pixel in the earlier exposure, the integration time in the earlier exposure, and the time since that exposure. In this model, the amplitude of the persistence varies slowly across the face of the detector, but the other properties are (to first order) independent of the location on the detector. This program will obtain a better measure of these amplitude variations, so that the correction flat used in the model can be made more accurate. The data will also be used to test more rigorously whether there are spatial variations that depend on properties such as exposure time or degree of saturation of the image responsible for generating persistence. The observations consist of a series of Tungsten lamp exposures followed by darks. Seven filters are used to achieve 5 fluence levels, each with a range of four exposure lengths.

IDs:	14380 (Cycle 23)
ISRs:	ISR 2018-03: Persistence in the WFC3 IR Detector: Intrinsic Variability

❖ IR Persistence: Position-Dependent Model

Purpose: 1.) Develop the first spatially-dependent model of persistence for the IR detector, 2.) Investigate how persistence can be reactivated following exposures with Tungsten lamp.

Description: Each visit begins with a series of 4 dark exposures to establish the dark level, a single exposure of a field in Omega Centauri, a series of darks to measure the persistence after the Omega Centauri exposure, a Tungsten lamp exposure to activate additional persistence, and a follow-up series of darks to measure the induced (reactivated) persistence. Combined with data from prior calibration programs, the Omega Centauri exposures provide enough data to create a spatially varying model in a 4x4 grid at 6 different exposure times (149, 274, 499, 599, 899, and 1199 seconds). Tungsten exposures toward the end of the visit are intended to reactivate persistence, and this program will investigate the level of saturation required to reactivate persistence how this induced signal decays with time.

IDs:	14381 (Cycle 23)
ISRs:	ISR 2018-04: Persistence in the WFC3 IR Detector: An Area Dependent Model

3.) Photometry

❖ UVIS Supplemental Photometry: Color Terms and Revisiting M512C

Purpose: 1.) Measure any color-dependence in the inverse sensitivity for UV filters (F218W, F225W, F275W) as a function of spectral type and position on the detector. 2.) Check the accuracy of the photometric calibration near the middle of the FOV where most users place their targets, as this region has not been observed via the photometric monitoring program since 2012.

Description: To characterize any spatial dependence in the UVIS color terms, two white dwarfs (GD71 and GD153), an A star (1812095, a CALSPEC standard), and a G star (P330E) are observed in the 4 corner subarrays for the three UV filters plus F606W and F814W to reach a SNR ~ 200 . Current F275W observations of GD153 and P330E show color terms $\sim 2\%$ at the same position on the detector, while synthetic and observed photometry show that the color effect across UVIS chips may differ by up to 3-6% according to filter. To recheck the absolute photometric calibration at the center of the UVIS array, the two white dwarfs, the A-star, and the G star are observed in 10 filters with the M512C subarray to achieve a SNR ~ 500 .

IDs:	15399 (Cycle 25)
ISRs:	ISR 2018-08: WFC3 color term transformations for UV filters ISR 2016-05: UVIS 2.0: Ultraviolet Flats

❖ Improved Precision, Wavelength Dependence of the IR CRNL

Purpose: Extend the range and precision of the IR channel count rate non-linearity (CRNL) to very faint objects and test for any significant wavelength dependence, similar to that found for NICMOS.

Description: The absolute photometric calibration was performed using bright (11th mag) white dwarf standards. This program will test the accuracy of applying these zeropoints to very faint objects (at the sky count-rate $\sim 23^{\text{rd}}$ mag). The present uncertainty in CRNL is 0.01 mag/dex (factor of 10), and a difference of 12 magnitudes is 4.5 dex making the uncertainty for faint objects up to 0.045 mag. The goal of the new data is to improve the uncertainty to 0.01 mag at 23^{rd} mag. This is achieved by doubling the dynamic range of the data (using two exposure times, short and long) and by observing an outer field in 47 Tucanae, which is more rich in stars than NGC 3603 (from the WFC3/ERS program 11360) but not as crowded as the Omega Centauri data obtained in Cycle 19 (program 12700). Because the UVIS F850LP and IR F098M filters

cover such similar wavelengths, the linearity of the UVIS detector (in F850LP), with a small color term (F775W-F850LP), can be used to test the CRNL of the IR detector (in F098M). Observations in F125W and F160W may then be ‘bootstrapped’ off the F098M filter to check for any dependence of the CRNL with wavelength.

IDs:	14868 (Cycle 24), 12700, 12335, 11933, 11360
ISRs:	ISR 2011-15: An Independent Determination of WFC3-IR Zeropoints and Count Rate Non-Linearity from 2MASS Asterisms ISR 2010-15: Boosting Count-rates with Earth Limb Light and the WFC3/IR Count-rate Non-linearity ISR 2010-07: First On-orbit Measurements of the WFC3-IR Count-rate Non-Linearity NICMOS ISR 2006-003: Correcting the NICMOS count-rate dependent non-linearity NICMOS ISR 2006-002: NICMOS Count Rate Dependent Non-Linearity in G096 and G141 NICMOS ISR 2006-001: NICMOS Count-rate Dependent Non-linearity Tests using Flatfield Lamps NICMOS ISR 2005-002: Grism Sensitivities and Apparent Non-Linearity

❖ IR Zeropoint Linearity

Purpose: Check the linearity of the WFC3/IR inverse sensitivity (photometric zeropoints) using faint HST standard stars and compare with the results derived from bright standards.

Description: The photometric monitoring program observes bright white dwarf and G-type flux standards for routine monitoring of the detector response. The zeropoints are therefore computed for sources with high count rates and short exposure times. IR detectors are non-linear devices, thus zeropoints for faint sources may be different compared to those derived from bright stars. The addition of the faint CALSPEC white dwarf WD1657+343 and the faint G-star SNAP-2 increases the total dynamic range to ~250 with respect to the bright white dwarf standards. Including observations of the bright M-star VB8 (GJ644C) from Cycles 18 and 22 increases the dynamic range to ~500 for wavelengths greater than 1 micron.

IDs:	14870 (Cycle 24), 14021, 12334
ISRs:	Rubin et al. (2015) AJ, 149, A Calibration of NICMOS Camera 2 for Low Count Rates ISR 2011-15: An Independent Determination of WFC3-IR Zeropoints and Count Rate Non-Linearity from 2MASS Asterisms ISR 2010-07: First On-orbit Measurements of the WFC3-IR Count-rate Non-Linearity

❖ Improving the CALSPEC model for GRW+70D5824

Purpose: Improve GRW+70D5824 (GRW) as a flux standard by obtaining precise (high signal to noise) STIS spectroscopy between 0.3 and 1.0 microns. The goal of providing end-to-end flux calibration with errors $\sim 1\%$ means that all various sub-pieces must be defined to sub-percent precision. In addition to providing a new excellent flux standard for the community, there are dozens of existing ACS and WFC3 observations that would become useful for cross-instrument flux calibration in the crucial 3000-5500 Å range.

Description: GRW is frequently observed by WFC3, ACS and STIS in the UV to monitor contamination and PSF (focus) changes, however this star is not yet a good CALSPEC flux standard. Its lone G430L STIS spectrum, used to establish the absolute flux between 3000-5500 Å and which covers some of the most important filters for ACS and WFC3, is of poor quality with uncertainties $\sim 2\text{-}3\%$. Three high signal-to-noise STIS spectra in G430L are required to reduce the statistical noise to $< 1\%$. Further, there are only two epochs of G750L spectra (5240-10270 Å), resulting in uncertainties at a level of $\sim 1.1\%$. By combining additional STIS observations with the existing 86 G140L (1150-1730 Å) and 89 G230L (1570-3180 Å) spectra, GRW will become one of the five best CALSPEC standards with complete STIS and NICMOS coverage to 2.5 microns and errors $< 1\%$ over the full wavelength range.

IDs:	14871 (Cycle 24)
ISRs:	Bohlin, Gordon, & Tremblay 2014 PASP, Vol. 126, No. 942, Techniques and Review of Absolute Flux Calibration from the Ultraviolet to the Mid-Infrared Bohlin, Dickinson, & Calzetti 2001, AJ, 122, 2118, Spectrophotometric Standards From Far-UV To Near-IR: STIS & NICMOS Fluxes HST CALSPEC database: http://www.stsci.edu/hst/observatory/crds/calspec.html

4.) UVIS Detector

❖ UVIS Sink Pixel Map Update

Purpose: Identify when and where new sink pixels have formed, measure their impact as a function of the image background, and update the UVIS sink pixel mask accordingly.

Description: A unique type of chip defect, “sink pixels” contain an atypically high number of CTE traps. As a consequence, sink pixels appear as effectively delta-functions in high-background images and as long troughs in low background images. As of mid-2014, about 0.05% of WFC3/UVIS pixels were identified as sinks deeper than 20 electrons; including the

troughs, up to 0.5% of pixels are impacted by sinks. These defects are currently flagged in the CTE-correction branch of calwf3 via the use of a sink pixel mask. However, the number of sink pixels is known to increase with time, likely because they are a result of radiation damage. Thus there is a need to inventory the current sink pixel population and propagate the results to the pipeline. For this program, ten short darks were obtained at four post-flash levels [25 e⁻, 50 e⁻, 100 e⁻, 200 e⁻] to understand the effect of different background levels.

IDs:	14879 (Cycle 24), 13638 (Cycle 21)
ISRs:	ISR 2014-19: Sink Pixels and CTE in the WFC3/UVIS Detector ISR 2014-22: Flagging the Sink Pixels in WFC3/UVIS

5.) CTE

❖ UVIS CTE Model Recharacterization

Purpose: Construct an updated empirical model of the UVIS CTE using a series of short darks with various levels of post-flash.

Description: The current UVIS pixel-based CTE model was developed from calibration observations obtained in 2014. Now that UVIS has spent almost twice as much time on-orbit, CTE losses should be ~2x as bad, with ~twice as many warm pixels (WPs). This program will obtain a series of short (50 second) dark exposures at a variety of post-flash levels (from 1-300 electrons). The long (900 second) darks needed for this analysis will come from the standard ‘Daily Monitor’ program (14531), which uses a ‘moderate’ post-flash level of 12 electrons. Any differences can be traced to CTE: the loss of flux in the WPs help quantify the CTE losses, and the trails tell where the flux went. These data will be used to re-evaluate the CTE correction model to ensure that the parameters are measured as accurately as possible and that 12 electrons remains an optimal post-flash level for science observations. The CTE behavior in subarrays will be compared to full-frame exposures to evaluate any dependence on the readout timing.

IDs:	14880 (Cycle 24), 13567 & 13568 (Cycle 21)
ISRs:	ISR 2014-19: Sink Pixels and CTE in the WFC3/UVIS Detector Anderson et al. 2012, The Efficacy of Post-Flashing for Mitigating CTE Losses in WFC3/UVIS Images Anderson et al., 2012, AAS, 220, 136.10, Fitting a Pixel-Based CTE Model to the WFC3/UVIS CCD Detector Baggett et al. 2011, WFC3 UVIS CTE Whitepaper

❖ UVIS CTE Pixel-Based Model Evaluation

Purpose: Evaluate CTE losses in a stellar field as a function of background level to assess the ability of the ‘revised’ pixel-based reconstruction algorithm (derived using short and long darks obtained in program 14880) to correct the images.

Description: Using observations of the Galactic bulge, provide a direct evaluation of the efficacy of the improved pixel-based correction, in terms of photometry, astrometry, *and* shape. This program takes four deep (800 second) exposures and 8 short (40 second) exposures with identical positions and a range of backgrounds so that the pixel-based, CTE-corrected short exposures can be compared with the “truth” from the deep set of exposures.

IDs:	14881 (Cycle 24)
ISRs:	ISR 2016-01: The Updated Calibration Pipeline for WFC3/UVIS: A Reference Guide to Calwf3 3.3 ISR 2014-19: Sink Pixels and CTE in the WFC3/UVIS Detector

6.) Grisms

❖ WFC3 -1st Order IR Grism Calibration

Purpose: Improve the flux calibration and correct and map the sensitivity curve of the -1st orders of the G102 and G141 filters to enable accurate and precise spectroscopic observations of bright targets.

Description: One external orbit for each of the two IR grisms will be used to obtain -1st order spectra with signal-to-noise ~100 of the brightest photometric standard star, 1802271, at five positions on the detector. Observations of P330E in the G141 -1st order showed that the sensitivity curve is incorrect; therefore high signal-to-noise spectra of this A-type standard star are needed to correct the shape, consistent with measurements for the +1st orders.

IDs:	14388 (Cycle 23), 13094, 12336
ISRs:	ISR 2014-15: Enabling Observations of Bright Stars with WFC3 IR Grisms

7.) Astrometry

❖ Astrometric Verification of Broad, Medium, Narrow, and Quad UVIS Filters

Purpose: Calibrate the filter-dependent component of the geometric distortion with <0.1 pixel precision for all previously unobserved UVIS filters by obtaining dithered observations of the standard astrometric field in Omega Centauri. Additional observations in the F606W filter are used to monitor the stability of the distortion over time.

Description: Observations of Omega Centauri in 14 broad and medium filters obtained in prior calibration cycles show that in addition to the high-order polynomial distortion and the UVIS lithographic mask pattern (corrected via the IDCTAB and D2IMFILE reference files), there are additional small-scale residual distortions ~ 0.2 pixel in virtually all filters. These may be corrected using a two-dimensional look-up table (NPOLFILE) for each filter. In this cycle, a grid of either five or nine dithered exposures offset by $\pm 40''$ are obtained in a given UVIS filter, followed by a single exposure in the F606W reference filter. This new program acquires observations in 5 broad (F200LP, F218W, F300X, F475X, F600LP), 6 medium (F410M, F467M, F547M, F689M, F763M, F845M), 11 narrow (F280N, F343N, F373N, F395N, F469N, F487N, F502N, F631N, F645N, F665N, F680N), and 3 quad (FQ378N, FQ492N, FQ937N) filters in order to correct for any filter-dependent structure.

IDs:	14393 (Cycle 23)
ISRs:	ISR 2018-10: Updates to the WFC3/UVIS Filter-Dependent Geometric Distortion ISR 2014-12: Astrometric Correction for WFC3/UVIS Filter-Dependent Component of Distortion

❖ Time-Dependence of X-CTE and Astrometry

Purpose: Improve the measurement of X-CTE and its effect on high-precision astrometry and measure any time evolution from calibration data obtained in the previous cycle.

Description: To measure local variations in the accuracy of the geometric distortion solution, Cycle 22 program 13929 obtained scanned observations of M48 (in F621M and F673N) and M67 (in F606W), with sequential exposures dithered in the X-direction by a large fraction of the field of view. These three filters span different magnitude ranges, allowing a probe of the X-CTE effect from $V=7$ to $V=16$. Dithered pairs of exposures in which a bright line (scanned star)

crosses the x=2048 pixel mid-line show systematic differences from the expected positions of ~0.0015 pixels for bright stars and ~0.0040 pixels for faint stars. This Cycle 23 program obtains 10 additional pairs of dithered observations to more precisely constrain the effect of X-CTE on the measured position of sources. Using these data, a static correction to the geometric distortion solution may be computed for science programs which require high-precision astrometry.

IDs:	14394 (Cycle 23), 13929, 13571, 13101
ISRs:	ISR 2014-02: The Impact of x-CTE in the WFC3/UVIS detector on Astrometry Casertano et al. (2016) ApJ, 825, “ Parallax of Galactic Cepheids from Spatially Scanning the Wide Field Camera 3 on the Hubble Space Telescope: The Case of SS Canis Majoris ”

IV. Routine Calibration

The majority of WFC3 calibration programs provide routine monitoring for the UVIS and IR channels. These calibrations have been obtained continuously since WFC3 was installed in 2009 during Servicing Mission 4 and typically do not change strategy between cycles. These monitors may be divided into seven main categories: UVIS Detector, UVIS CTE, IR Detector, Grisms, Photometry, Flat Fields and Astrometry. Table 4 lists the 23 routine programs repeated each cycle, color coded by topic, along with the standard orbit allocation. Note that this table does not include ‘IR Persistence’, for which the calibration strategy changes from cycle-to-cycle, nor does it contain the new ‘PSF/Focus’ category in Table 3 which was added in Cycle 26.

In this section, a detailed description of each monitoring program is provided, along with an overview of the observing strategy. Additionally, a list of all proposal IDs to date and a complete list of Instrument Science Reports (ISRs) related to each calibration program are given in reverse chronological order. Considering the large number of calibration ISRs published over the WFC3 lifetime, these are not individually cited in the ‘References’ section of this report, but are instead provided as direct links to the PDF files.

Table 4. WFC3 calibration monitoring programs which are repeated every cycle. Rows are color coded by topic: UVIS Detector Monitoring (blue), UVIS CTE Characterization (yellow), IR Detector Monitoring (red), Grism Calibration (purple), Photometry (green), Flat fielding (light blue), and Astrometric Calibration (orange). The typical external and internal orbit allocation per cycle is indicated in the last two columns.

Topic	Program Title	External Orbits	Internal Orbits
UVIS Detector	UVIS Anneal	0	79
	UVIS Bowtie Monitor	0	132
	UVIS CCD daily Monitor	0	642
	UVIS CCD Unflushed Monitor	0	130
	UVIS Post-Flash Monitor	0	60
	UVIS CCD Gain Stability	0	18
UVIS CTE	UVIS CTI Monitor (EPER)	0	12
	UVIS CTE Monitor (star cluster)	8	0
	Characterization of UVIS traps with Charge Injection	0	36
IR Detector	IR dark monitor	0	97
	IR linearity monitor	0	10
	IR gain monitor	0	16
Grisms	IR Grism Wavelength Calibration & Stability	1	0
	IR Grism Flux/Trace Calibration & Stability	1	0
	UVIS Grism Wavelength Calibration & Stability	1	0
Photometry	UVIS shutter monitoring	0	1
	WFC3 UVIS & IR photometry	12	0
	UVIS contamination monitor	20	0
Flat Fields	UVIS Pixel-to-Pixel QE Variations via Internal Flats	0	45
	UVIS internal flats	0	13
	IR internal flats	0	18
	WFC3 CSM monitor with Earth flats	0	200
Astrometry	WFC3 Astrometric Scale Monitoring	6	0

1.) UVIS Monitoring

❖ UVIS Anneal

Purpose: Perform regular anneal procedures to 1) repair hot pixels and 2) acquire internal exposures to assess the anneal's effectiveness as well as produce reference files for the calibration pipeline.

Description: WFC3 anneals are performed every 28 days, a cadence which interleaves the WFC3 procedure with those from other instruments, one instrument per week. Internal biases as well as darks are taken before and after each procedure to provide a check of bias level, read noise, global dark current, and hot pixel population. A bowtie visit is acquired immediately after each anneal to provide a hysteresis-neutralizing image as well as verify that any hysteresis present has been successfully quenched. Each iteration requires 6 orbits (2 before and 2 after each anneal for biases/darks + 1 orbit for the anneal itself + 1 orbit for the attached post-anneal bowtie visit).

IDs:	12343, 12687, 13071, 13554, 14000, 14366, 14529, 14978, 15567
ISRs:	ISR 2017-23: WFC3/UVIS: Bias Reference Files Analysis ISR 2017-17: WFC3/UVIS Read Noise Aug 2009 - Apr 2017

❖ UVIS Bowtie Monitor

Purpose: Condition the UVIS detector for science observing. During TV internal flat testing, it was discovered that the UVIS detector exhibits occasional low-level (~1%) quantum efficiency offsets (i.e. hysteresis) across both chips, an effect dubbed 'bowtie' due to its unique shape in the image ratios. The ground tests revealed that hysteresis can be negated by overexposing the detector by several times the full well. This monitoring program was developed to detect and mitigate UVIS hysteresis on orbit.

Description: Each visit acquires a set of three 3x3 binned internal Tungsten flats obtained every three days in the F475X filter. These include (1) an unsaturated image to check for hysteresis features, (2) a saturated 'QE pinning' exposure to fill traps and mitigate QE offsets, and (3) an additional unsaturated image to assess the hysteresis removal efficiency. The F475X filter was selected for (1) its high throughput, (2) its bandpass (<700nm), which is known to mitigate hysteresis and (3) its status as a low-priority filter for science observations.

IDs:	12344, 12688, 13072, 13555, 14001, 14367, 14530, 14979, 15568
ISRs:	ISR 2018-11: UVIS Flat Fields Affected by Shutter-Induced Vibration ISR 2017-08: Monitoring the WFC3/UVIS Relative Gain with Internal Flatfields ISR 2013-09: WFC3/UVIS Bowtie Monitor ISR 2009-24: WFC3 SMOV Proposal 11808: UVIS Bowtie Monitor

❖ UVIS CCD Daily Monitor

Purpose: Monitor the behavior of the UVIS CCDs with a daily set of bias and/or dark frames. These data will be used to generate bias and dark reference files for CRDS. These reference files are used to calibrate all WFC3/UVIS images.

Description: The internals are acquired using a pattern of single-orbit visits repeated every 4 days. All darks are 900 seconds in duration and all exposures are post-flashed. Day 1: two visits (one with 2 biases, one with 2 darks). Day 2: two visits (2 darks each). Day 3: one visit (2 darks). Day4: two visits (2 darks each). Starting in Cycle 22, the Daily monitor was split into 3 smaller consecutively numbered programs for easier scheduling.

IDs:	12342, 12689, 13073, 13556, 14002/03/04, 14368/69/70, 14531/32/33, 14980/81/82, 15569/70/71
ISRs:	ISR 2017-23: WFC3/UVIS: Bias Reference Files Analysis ISR 2016-08: WFC3/UVIS Dark Calibration: Monitoring Results and Improvements to Dark Reference Files ISR 2014-04: WFC3 Cycle 19 & 20 Dark Calibration: Part I ISR 2015-13: WFC3 UVIS Read Noise

❖ UVIS Unflushed CTE Monitor

Purpose: Obtain un-flashed darks to monitor how well the post-flash is mitigating CTE and to measure the growth of hot pixels observed exposures with low background.

Description: Temporal changes in CTE losses and the efficacy of the post-flash mode are monitored by a series of WFC3/UVIS darks (with no post-flash) taken before and after the monthly UVIS anneal. A large number of internals are taken as part of a daily monitor of warm/hot pixel growth and read noise, however they are all post-flashed. Thus, a small number of un-flashed internals are required to monitor the changes in CTE losses over with time. When

used conjunction with the post-flashed internals, the un-flashed internals allow for an assessment of how well the post-flash is mitigating the CTE losses.

IDs:	13559, 14005, 14371, 14534, 14983, 15572
ISRs:	In preparation

❖ UVIS Post-Flash Monitor

Purpose: Monitor the flux and illumination pattern of the post-flash LED over time. The data are used to also create a series of post-flash reference files for the calibration pipeline.

Description: Most observers with low-background ($< 12 e^-$) data are now using the post-flash mode in WFC3/UVIS. This program continues the monthly monitoring of the lamp characteristics, with additional orbits to allow new generation of post-flash reference files. Each monthly iteration of the monitor requires 3 orbits: two to obtain high S/N flashed full-frames for both shutter blades (to check for pattern changes) and one to obtain a 1k x1k subarray at a variety of flash levels (to check on the brightness stability of the lamp). For the new reference files, 12 orbits are needed. In the event the LED illumination pattern changes more rapidly than expected, 12 additional orbits would be needed.

IDs:	13078, 13560, 14006, 14372, 14535, 14984, 15573
ISRs:	ISR 2017-13: Generating the WFC3 UVIS Post-Flash Reference File ISR 2017-03: Long-term Stability of the Post-Flash LED Lamp ISR 2013-12: WFC3 Post-Flash Calibration ISR 2003-01: Minimizing CTE losses in the WFC3 CCDs: Post Flash vs. Charge Injection

❖ UVIS Gain Stability

Purpose: Monitor the absolute gain for the nominal detector count using the mean-variance technique.

Description: Observations consist of 8 pairs of full-frame binned (2x2 and 3x3) and un-binned internal flats at nominal gain in the F645N filter with varying exposure times. Two epochs, at 9 orbits each, are taken ~6 months apart. Six of these orbits are for sampling the un-binned mode at lower signal levels.

IDs:	11906, 12346, 12690, 13168, 13561, 14007, 14373, 14536, 14985, 15574
ISRs:	ISR 2016-13: WFC3 Cycle 23 Proposal 14373: UVIS Gain ISR 2016-09: WFC3 Cycle 22 Proposal 14007: UVIS Gain ISR 2015-05: WFC3 Cycle 21 Proposal 13561: UVIS Gain ISR 2014-05: WFC3 Cycle 20 Proposal 13168: UVIS Gain ISR 2013-02: WFC3 Cycle 19 Proposal 12690: UVIS Gain ISR 2011-13: WFC3 Cycle 17 Proposal 11906: UVIS Gain ISR 2009-29: WFC3 SMOV Proposal 11419: UVIS Gain

2.) UVIS Charge Transfer Efficiency

❖ UVIS CTI Monitor

Purpose: 1.) Measure the UVIS CCD Charge Transfer Inefficiency (CTI) using the Extended Pixel Edge Response (EPER) method. 2.) Assess CTE losses over time in a continuation of the multi-cycle CTE monitor.

Description: Every other month, assess the profiles of excess charge in the extended pixel region of the special EPER readout format and monitor the CTI of the UVIS detector. Each epoch consists of two visits, each of which obtain an internal lamp flat field at a variety of illumination levels plus two short dark exposures to be used as a bias measurement.

IDs:	11924, 12347, 12691, 13082, 13565, 14011, 14377, 14540, 14989, 15575
ISRs:	ISR 2016-10: WFC3/UVIS EPER CTE Cycles Aug 2009 - Apr 2016 ISR 2013-03: WFC3/UVIS EPER CTE Measurement: Cycles 19 & 20 ISR 2011-17: WFC3/UVIS CTE-EPER Measurement: Cycle 17 & 18 ISR 2009-10: WFC3/UVIS CTE-EPER Measurement

❖ UVIS External CTE Monitor: Star Clusters

Purpose: Monitor CTE degradation as a function of epoch and source/observation parameters. Calibrate photometric corrections. Provide data to test and monitor the pixel-based CTE model.

Description: Starting in Cycle 25, post-flash is used to sample various background levels and monitor the efficacy of the post-flash model for CTE mitigation. Exposures of NGC 6791 and 47

Tucanae in F502N (~zero background) will monitor the maximum CTE in different field densities. Long exposures, dithered by 2000 pixels in detector Y, will measure absolute CTE. Various background levels are sampled to test whether the currently recommended level of 12 electrons still yields the best charge transfer. The data are also used to test the effectiveness of the pixel-based CTE correction software. Observations are obtained twice per year and comprise 4 orbits per epoch.

IDs:	12379, 12692, 13083, 13566, 14012, 14378, 14541, 14990, 15576
ISRs:	ISR 2017-09: WFC3/UVIS External CTE Monitor: 2016 Updates on Coefficients and Analysis Pipeline ISR 2016-17: WFC3/UVIS External CTE Monitor: Single-Chip CTE Measurements ISR 2015-03: WFC3/UVIS Charge Transfer Efficiency 2009 - 2015 ISR 2012-09: WFC3 UVIS Charge Transfer Efficiency October 2009 to October 2011 ISR 2011-06: WFC3/UVIS-Cycle 17: CTE External Monitoring-NGC 6791

❖ Characterization of UVIS Traps with Charge Injection

Purpose: Monitor the growth of UVIS traps via charge-injected biases.

Description: The charge transfer efficiency (CTE) of the WFC3/UVIS channel continues to decline as damage from radiation accumulates. One method to mitigate the impact of CTE losses is to apply a pixel-based CTE correction algorithm the images after they are acquired. An algorithm such as this requires a detailed knowledge of the traps, which capture and release charge during the image readouts. This program will identify and characterize the traps responsible for the charge losses, map their distributions across the chips, and monitor their growth over time. One orbit of ‘line 25’ charge-injected biases are obtained every ~10 days.

IDs:	12348, 12693, 13084, 13569, 14013, 14379, 14542, 14991, 15577
ISRs:	ISR 2011-02: WFC3/UVIS Charge Injection Behavior: Results of an Initial Test

3.) IR Monitoring

❖ IR Dark Monitor

Purpose: Acquire a variety of IR darks to support the removal and study of dark current. SPARS200 dark observations are periodically obtained to monitor trends in the bad pixels (hot, unstable, or dead), zeroth read level, and dark current. The remaining orbits collect dark ramps for generating stacked IR dark calibration reference files.

Description: Full-frame and subarray dark images will be collected using each sample sequence. The total number of images collected over the course of the cycle for a given mode is based on the total number of input ramps used in the current superdark for that mode and the popularity of that mode in external science observations. The IR dark current has remained nearly unchanged since launch which allows for more relaxed scheduling constraints compared to older WFC3/IR dark monitor programs. Twenty-six orbits of SPARS200 darks are obtained every 2 weeks + 71 orbits spread amongst the other 23 sample sequence/subarray combinations (weighted by usage). An 1800 second, non-interruptible hold precedes the observations to protect from IR persistence.

IDs:	11929, 12349, 12695, 13077, 13562, 14008, 14374, 14537, 14986, 15578
ISRs:	ISR 2017-24: A Predictive WFC3/IR Dark Current Model ISR 2017-04: An Exploration of WFC3/IR Dark Current Variation ISR 2014-06: New WFC3/IR Dark Calibration Files ISR 2012-11: WFC3/IR Dark Current Stability

❖ IR Linearity Monitor

Purpose: Monitor the non-linearity of the IR detector and track the stability over time.

Description: HgCdTe detectors suffer from a non-linear response to incident flux, and the calibration pipeline corrects for the effects of non-linearity. This monitor uses flat field ramps to characterize the non-linearity of each detector pixel via 10 internal orbits, executed once per year. Each orbit is identical in structure and consists of a dark observation followed by two internal flats using the Tungsten lamp through F126N (half SPARS10, half SPARS50) and F127M (half SPARS25, half SPARS10). The initial narrow-band flat is used to ensure that the lamp is warm and stable in preparation for the F127M exposure, but not so bright to cause persistence. A trailing dark is obtained after the F127M flat to measure the persistence decay rate.

IDs:	12352, 12696, 13079, 13563, 14009, 14375, 14538, 14987, 15579
ISRs:	ISR 2014-17: Updated non-linearity calibration method for WFC3/IR ISR 2008-39: WFC3 TV3 Testing: IR Channel Nonlinearity Correction

❖ IR Gain Monitor

Purpose: Measure the gain in the four quadrants of the IR detector twice per year.

Description: The relation between analog digital units (ADU) and photo-electrons is a fundamental detector parameter. Gain can be measured using the mean-variance method on pairs of internal flats. For each quadrant of the ramp pairs, the mean-variance method is used to calculate the gain. Eight internal orbits are obtained ~6 months apart. Each visit is identical and begins with a dark, allowing the BLANK to move into position before the lamp is turned on. The Tungsten lamp is turned on, and while the lamp warms a short flat is taken through F126N to ensure a linear signal hits the detector for the duration of the long flat. Next, the long flat field ramp to be used in the gain measurement is obtained. Finally, a trailing dark is obtained to monitor persistence. Pairs of ramps are observed within 24 hours.

IDs:	11930, 12350, 12697, 13080, 13564, 14010, 14376, 14539, 14988, 15580
ISRs:	ISR 2015-14: WFC3 IR Gain from 2010 to 2015 ISR 2008-50: WFC3 TV3 Testing: IR Gain Results

4.) Grism Calibration

❖ IR Grism Wavelength Calibration and Stability

Purpose: Verify the temporal stability of the wavelength dispersion for the G102 and G141 IR grisms.

Description: Observations of VY2-2 are used to verify that the dispersion of these grisms is not changing. Starting in Cycle 25, only a single pointing at the center of the detector is obtained for each grism G102 and G141. (Prior cycles used multiple detector pointings to calibrate the spatial variability of the wavelength dispersion relation.)

IDs:	12356, 12703, 13093, 13580, 14023, 14385, 14543, 14543, 14993, 15586
ISRs:	ISR 2017-01: A More Generalized Coordinate Transformation Approach for Grisms ISR 2016-15: Trace and Wavelength Calibrations of the G102 and G141 IR Grisms ISR 2015-10: IR Grism Wavelength Solutions Using the Zero Order Image as the Reference Point

❖ IR Grism Flux/Trace Calibration and Stability

Purpose: Verify the temporal stability of the trace solution and flux calibration for the G102 and G141 grisms.

Description: Observations of GD-153 are used to verify that the dispersed traces of these grisms are not changing and that the sensitivity remains stable. Starting in Cycle 25, only a single pointing at the center of the detector is obtained for for each grism G102 and G141. (Prior cycles used multiple detector pointings to calibrate the spatial variability.)

IDs:	12357, 12702, 13092, 13579, 14024, 14386, 14544, 14994, 15587
ISRs:	ISR 2016-15: Trace and Wavelength Calibrations of the G102 and G141 IR Grisms

❖ UVIS Grism Wavelength Calibration and Stability

Purpose: Verify and refine the UVIS wavelength calibration, as necessary. These calibration data will improve our ability to process currently archived data as well as support current and future UVIS parallel observations.

Description: Spectra of WR-14 with the G280 grism are used to verify that the dispersion of this grism is not changing. This calibration supports the HST UV initiative. One orbit is used to obtain 4 pointings (2 per chip). The positions will repeat the previously observed positions (critical as they show +1 and -1 orders) and verify the stability of this mode.

IDs:	12359, 12705, 13091, 13578, 14025, 14387, 14545, 14995, 15588
ISRs:	ISR 2017-20: Trace and Wavelength Calibrations of the UVIS G280 +1/-1 Grism Orders ISR 2011-18: First Results from Contamination Monitoring with the UVIS G280 Grism ISR 2009-01: The ground calibrations of the WFC3/UVIS G280 grism

5.) Photometric Calibration

❖ UVIS Shutter Monitoring

Purpose: Monitor the performance of the UVIS shutter blades. The specific objectives are to compare the photometric behavior of both shutter blades (for short vs long exposures) and to check for any shutter shading effects.

Description: Internal flats with the tungsten lamp in each of the 4 amps are used to monitor the repeatability and any shutter shading effects. The photometric behavior of blades A and B will continue to be monitored separately. Internal flats from the bowtie monitoring program provide an additional check of the shutter repeatability. Standard star observations from Cycles 23 & 24 show no noticeable difference in the performance of the shutter compared to SMOV, so no external orbits were requested in Cycles 25 and 26.

IDs:	11427, 14019, 14383, 14882, 15397, 15584
ISRs:	ISR 2018-11: UVIS Flat Fields Affected by Shutter-Induced Vibration ISR 2015-12: WFC3/UVIS Shutter Characterization ISR 2014-09: Use of the Shutter Blade Side “A” for UVIS Short Exposures ISR 2009-25: UVIS Channel Shutter Shading

❖ UVIS and IR Photometry

Purpose: Monitor the photometric throughput and stability, measure the inverse sensitivities and determine color term corrections for UVIS and IR filters as a function of time, detector position, and wavelength.

Description: For the UVIS detector observe three white dwarf standards (GD71, GD153, GRW+70) and a G-type star (P330E) in a subset of broad- and medium-band filters using the corner subarrays. In Cycle 26, GRW+70 replaces G191B2B, which is too bright in many UVIS filters and which is not used for the IR photometric calibration. An improved spectrum of GRW+70 was recently added to CALSPEC in August 2017 based on new STIS data from Cy24 (program 14871). This new target also allows for better synergy with the UVIS contamination program, which observes GD153 and GRW+70. For the IR detector, observe GD153, GD71 and P330E in all IR imaging filters. (G191B2B was dropped in Cy20 because it is too bright.) In Cycle 26, add 1 orbit of GRW+70 to reinstate a 3rd white dwarf and to provide overlap with the selected UVIS standards, which is important for cross-calibration of the two detectors.

IDs:	11450 (UVIS), 11451 (IR), 11903 (UVIS), 11926 (IR), 12334, 12699, 13089, 13575, 14021, 14384, 14871, 14883, 14992, 15582
ISRs:	<p>UVIS:</p> <p>ISR 2018-08: WFC3 color term transformations for UV filters</p> <p>ISR 2018-02: Comparing the ACS/WFC and WFC3/UVIS Calibration and Photometry</p> <p>ISR 2017-14: WFC3/UVIS Updated 2017 Chip-Dependent Inverse Sensitivity Values</p> <p>ISR 2017-07: WFC3 Chip Dependent Photometry with the UV filters</p> <p>ISR 2016-07: Updated WFC3/UVIS Chip Dependent SYNPHOT/PYSYNPHOT Files</p> <p>ISR 2016-03: UVIS 2.0 Chip-dependent Inverse Sensitivity Values</p> <p>ISR 2010-14: The Photometric Performance of WFC3/UVIS: Temporal Stability Through Year 1</p> <p>ISR 2009-38: WFC3 SMOV Programs 11436/8: UVIS On-orbit PSF Evaluation</p> <p>ISR 2009-31: WFC3 SMOV Proposal 11450: The Photometric Performance and Calibration of WFC3/UVIS</p> <p>IR:</p> <p>ISR 2011-08: The Photometric Performance of WFC3/IR: Temporal Stability Through Year 1</p> <p>ISR 2009-37: WFC3 SMOV Programs 11437/9: IR On-orbit PSF Evaluation</p> <p>ISR 2009-30: WFC3 SMOV Proposal 11451: The Photometric Performance and Calibration of WFC3/IR</p>

❖ UVIS Contamination Monitor

Purpose: Periodically measure the photometric throughput of the UVIS detector. These data monitor the presence of possible contaminants on the optics via the flux of standard stars as a function of time and wavelength.

Description: Each visit obtains dithered or scanned subarray observations of a white dwarf standard star on both UVIS chips through a sub-sample of filters (including staring mode w/ grism G280). The white dwarf standard GRW+70D5824 has been used for past monitors, and a second white dwarf (GD153) was added in Cycle 23 with equal weight. This target has an added benefit of being schedulable throughout the year in 1-Gyro mode. The monitor cadence is deliberately out of sync with the monthly anneals in order to sample any anneal-related phase. Ten visits are obtained every ~5 weeks with 2 orbits/visit in both staring and scanned mode (which has greater precision over staring mode) for each of the two stars.

IDs:	(Staring mode): 11426, 11907, 12333, 12698, 13088, 13574, 14018, 14382, 14815; (Scans): 14878; (Staring and scans): 15398, 15583
ISRs:	<p>ISR 2017-21: Photometric Repeatability of Scanned Imagery: UVIS</p> <p>ISR 2017-15: 2017 Update on the WFC3/UVIS Stability and Contamination Monitor</p> <p>ISR 2014-20: Update on the WFC3/UVIS Stability and Contamination Monitor</p>

6.) Flat Field Calibration

❖ UVIS Pixel-to-Pixel QE Variations

Purpose: Track the population of pixels that exhibit anomalous QE variations between anneals.

Description: This program obtains internal flats to monitor the randomly distributed population of pixels that exhibit anomalous QE variations between anneals, characterized by a sensitivity loss that is more pronounced in the blue than in the red. This population is unique for each anneal cycle and exhibits clustering in the UV. For the UV filters, 6 orbits with the Deuterium lamp are taken in F225W and F336W, 1 orbit every other month in the week before the anneal. For the visible filters, 3 orbits each anneal cycle (a week before the anneal, midway between anneals, and just after the anneal) are taken with the Tungsten lamp in F438W, F645N and F814W.

IDs:	13169, 13585, 14027, 14389, 14546, 14996, 15589
ISRs:	ISR 2014-18: Pixel-to-Pixel Flat Field Changes in WFC3/UVIS

❖ UVIS Internal Flats

Purpose: 1.) Track the stability of the pixel-to-pixel sensitivity in all UVIS filters by obtaining internal flat fields with the tungsten and deuterium lamps. 2.) Monitor the decay of the internal lamps.

Description: This program acquires internal flats in all UVIS filters once per year with the Deuterium lamp in the F218W, F200LP, F225W, F275W, F280N, F300X, F336W, F343N, F373N, F390M, F390W, F395N, FQ232N, FQ243N, FQ378N, and FQ387N filters and with the Tungsten lamp in the remaining 46 filters. Observations in F390W, F435W, F606W, and F814W will be repeated twice during the cycle.

IDs:	11432, 11914, 12337, 12711, 13097, 13586, 14028, 14390, 14547, 14997, 15590
ISRs:	ISR 2010-03: WFC3 SMOV Proposal 11432: UVIS Internal Flats

❖ IR Internal Flats

Purpose: 1.) Track the stability of the pixel-to-pixel sensitivity in all IR filters by obtaining internal flat fields with the tungsten lamp. 2.) Monitor the decay of the calibration lamps.

Description: This program measures the temporal and spatial stability of the IR flat field through all filters. High signal observations will provide a map of the pixel-to-pixel flat field structure and identify the positions of any dust particles. The full set of IR filters are sampled once in the middle of the cycle. A subset of broadband filters (F105W, F110W, F125W, F140W, and F160W) are obtained twice during the cycle (early and near the end). These data are used to update the bad pixel tables.

IDs:	11433, 11915, 12338, 12712, 13098, 13587, 14029, 14391, 14548, 14998, 15591
ISRs:	ISR 2015-11: The Internal Flat Fields for WFC3/IR ISR 2013-04: WFC3/IR Internal Flat Fields ISR 2009-42: WFC3 SMOV Program 11433: IR Internal Flat Field Observations

❖ WFC3 CSM Monitor with Earth Flats

Purpose: Monitor the CSM angle and new blob appearances using Earth flats.

Description: This program obtains short (~100 s) F153M exposures looking down at the dark Earth to use airglow as a uniform glowing screen. These images are used to detect new blobs and use the blob positions to track the CSM angle over time. At least one flat is acquired every time the CSM is moved, with a typical cadence of 1-2 times per week. (Gaps are expected when either the CSM doesn't move or the HST schedule is over-constrained.

IDs:	14392, 14549, 14999, 15592
ISRs:	ISR 2018-06: WFC3/IR Blob Monitoring ISR 2017-16: Possible Overlaps Between Blobs, Grism Apertures, and Dithers ISR 2015-06: The Impact of Blobs on WFC3/IR Stellar Photometry ISR 2014-21: Infrared Blobs: Time-dependent Flags ISR 2012-15: The WFC3 IR "Blobs" Monitoring ISR 2010-06: The WFC3 IR "Blobs"

7.) Astrometric Calibration

❖ WFC3 Astrometric Scale Monitoring

Purpose: Monitor the stability of the WFC3 geometric distortion over time.

Description: The standard astrometric catalog in the globular cluster Omega Centauri has been used to examine the geometric distortion of WFC3 as a function of wavelength on-orbit. The distortion coefficients implemented in the IDCTAB reference file are used in the HST pipeline to correct for ~7% distortion down to a level <1%. Observations in F606W (UVIS) and F160W (IR) are used to look for any time dependency and the effect of scale changes due to the thermal breathing. These observations may be used to derive the skew (non-perpendicularity of X&Y axis) and scale terms and look for any secular changes. Omega Centauri is observed three times during the year, with the same pointing in each detector, but with 3 different OTA roll-angles per orbit.

IDs:	11911, 12094, 12353, 12714, 13100, 13570, 14031, 14393, 14550, 15000, 15593
ISRs:	ISR 2018-10: Updates to the WFC3/UVIS Filter-Dependent Geometric Distortion ISR 2018-09: WFC3/IR: Time Dependency of Linear Geometric Distortion ISR 2018-01: Accuracy of the HST Standard Astrometric Catalogs ISR 2015-02: Standard Astrometric Catalog and Stability of UVIS Geometric Distortion ISR 2014-12: Astrometric Correction for WFC3/UVIS Filter-Dependent Component of Distortion ISR 2012-07: WFC3/UVIS and IR Multi-Wavelength Geometric Distortion ISR 2012-03: WFC3/UVIS and IR Time Dependency of Linear Geometric Distortion over Cycles 17 & 18 ISR 2009-34: WFC3 SMOV Proposal 11445 - IR Geometric Distortion Calibration ISR 2009-33: WFC3 SMOV Proposal 11444 - UVIS Geometric Distortion Calibration

V. Summary

A complete history of WFC3 calibration, both from ground testing and on-orbit, may be found on the 'Calibration Plan' webpage at <http://www.stsci.edu/hst/wfc3/calibration>. A separate page for each calibration cycle includes a list of Proposal IDs, titles, and direct links to the proposal information. As for all HST observing programs, the Phase II's (implementation) of these calibration proposals are public and may be found on the 'HST Program Status' webpage at http://www.stsci.edu/hst/scheduling/program_information.

The results from these calibration programs are published as they become available as Instrument Science Reports, which may be obtained from the ‘WFC3 ISRs’ webpage at <http://www.stsci.edu/hst/wfc3/documents/ISRs>. For the most recent calibration programs, an ISR may not yet be available, and the ‘Calibration Plan’ webpage includes a set of slides in PDF format highlighting the most recent reduction of the data. For the majority of monitoring programs, the data reduction and plots are generated automatically by WFC3 ‘Quicklook’ software.

Updated reference files will be provided to the scientific community when appropriate. These reference files will be automatically used by calwf3 to calibrate science observations when users retrieve their data from the HST archive. Otherwise, these files may be obtained via the ‘Calibration Reference Data System’ (CRDS) at <https://hst-crds.stsci.edu> for users who wish to manually recalibrate their observations. Instructions for manual recalibration are provided in the WFC3 Data Handbook (Gennaro et al. 2018).

Acknowledgements

The author is grateful to Elena Sabbi for reviewing this ISR and for sharing helpful insights from her time in the role as WFC3 Calibration Lead from Cycles 19 - 22. Thanks are also given to Sylvia Baggett who has been critical to the successful development and execution of numerous calibration programs, both on-orbit and also during ground testing activities dating back to 2003.

All calibration programs are developed and analyzed by the WFC3 team in the Instruments Division of STScI. Information in this report represents the cumulative experience and contributions of many members of the WFC3 Team, both past and present. At the time of this writing, the WFC3 team consists of Jay Anderson, Sylvia Baggett, Varun Bajaj, Gabriel Brammer, Matthew Bourque, Annalisa Calamida, Susana Deustua, Linda Dressel, Jules Fowler, Mario Gennaro, Harish Khandrika, Vera Khozurina-Platais, Heather Kurtz, Knox Long, Jennifer Mack, Catherine Martlin, Peter McCullough, Myles McKay, Jennifer Medina, Michele de la Pena, Norbert Pirzkal, Ryan Russell, Kailash Sahu, Clare Shanahan, Adam Riess, Elena Sabbi, Kevin Stevenson and Ben Sunnquist.

References

- Deustua S., et al. 2010, “WFC3 Cycle 17 Calibration Program”, WFC3 ISR 2009-08
- Deustua, S. 2011, “WFC3 Cycle 18 Calibration Program”, WFC3 ISR 2011-14
- Dressel, L. 2018, “WFC3 Instrument Handbook”, Version 10.0
- Gennaro, M. et al. 2018, “WFC3 Data Handbook”, Version 4.0
- Sabbi, E., et al. 2012, “WFC3 Cycle 19 Calibration Program”, WFC3 ISR 2012-04
- Sabbi, E., et al. 2013, “WFC3 Cycle 20 Calibration Program”, WFC3 ISR 2013-05
- Sabbi, E., et al. 2014, “WFC3 Cycle 21 Calibration Program”, WFC3 ISR 2014-07
- Sabbi, E., et al. 2015, “WFC3 Cycle 22 Calibration Program”, WFC3 ISR 2015-07